ELSEVIER

1 January 1998

Optics Communications 145 (1998) 329–339

OPTICS COMMUNICATIONS

Full length article

Lasing in diode-pumped Tm:YAP, Tm,Ho:YAP and Tm,Ho:YLF

I.F. Elder, M.J.P. Payne

DERA Malvern, St Andrews Road, Malvern, Worcs WR14 3PS, UK

Received 25 March 1997; revised 16 June 1997; accepted 1 July 1997

Abstract

A comparison of the room-temperature operation of continuous wave Tm:YAP, Tm,Ho:YAP and Tm,Ho:YLF lasers is reported. A conversion efficiency from absorbed pump power to laser output of 42% was demonstrated in Tm:YAP, compared to 14% in Tm,Ho:YAP and 30% in Tm,Ho:YLF. Tm:YAP was observed to operate multiline in the range 1.965 to 2.020 μm, whereas the holmium lasers operated on a single transition. The markedly different temporal behaviour of the single and double-doped crystals is analysed and discussed. © 1998 Elsevier Science B.V.

1. Introduction

Development of solid-state lasers operating in the two micron waveband has received considerable attention because of potential applications in a wide range of fields. Atmospheric remote sensing, which includes Doppler lidar wind sensing and water vapour profiling by differential absorption lidar, as well as altimetry and ranging are the principal areas of interest [1]. There are several medical applications requiring laser sources in the two micron waveband including arthroscopy, lithotripsy, orthopaedics and angioplasty [2–4]. Q-switched two micron lasers are useful as pump sources for optical parametric oscillators (OPOs) operating in the mid infrared spectral region [5,6].

The principal ions of interest are the triply charged rare earths thulium (Tm) and holmium (Ho) doped in glass or crystalline hosts, which operate as quasi-three level lasers. In these ions the lower laser level is a high-lying Stark level of the ground state energy level manifold, typically with a splitting in the range 300 to 600 cm^{-1}. Therefore the lower laser level has a temperature-dependent population determined by the Boltzmann distribution of population within the ground state energy level manifold.

The laser host YAP (chemical formula $YAlO_3$) is a biaxial crystal with the orthorhombic D_{2h}^{16} space group, the yttrium ions in sites of C_s (monoclinic) symmetry [7]. It is derived from the same Y_2O_3–Al_2O_3 system as the more common laser host YAG. However, although YAG is a mechanically robust oxide host, it has a cubic structure, which leads to thermal birefringence and consequent depolarisation losses when thermally loaded. The natural birefringence of YAP dominates any thermally induced birefringence which, combined with similar mechanical properties to YAG, makes it a potentially useful laser host. In addition, the emission cross-section of thulium in YAP is twice that of thulium in YAG; using the principle of reciprocity, absorption data yield thulium emission cross-sections of 6.0×10^{-20} cm^2 and 2.9×10^{-20} cm^2 in YAP and YAG respectively, in good agreement with published values [8]. The laser crystals used here were prepared from boules grown at DERA Malvern by the Czochralski technique, the growth direction being along the crystalline *b*-axis for YAP (Pbmn notation), and along the *a*-axis for YLF. Colour centre formation in the YAP during growth gave those boules an amber tint. No attempt was made to remove these colour centres by annealing the YAP boules, principally because with diode-pumping of thulium and holmium the presence of colour centres with absorption bands in the UV and visible does not impact upon lasing.

The thulium $^3H_6$ to $^3H_4$ absorption transition spans wavelengths overlapping the emission of high power GaAs/AlGaAs laser diodes. Fig. 1 depicts the room-temperature diode pump absorption bands of thulium in YAP and YLF. Temperature tuning of a single laser diode over

PII S0030-4018(97)00387-8

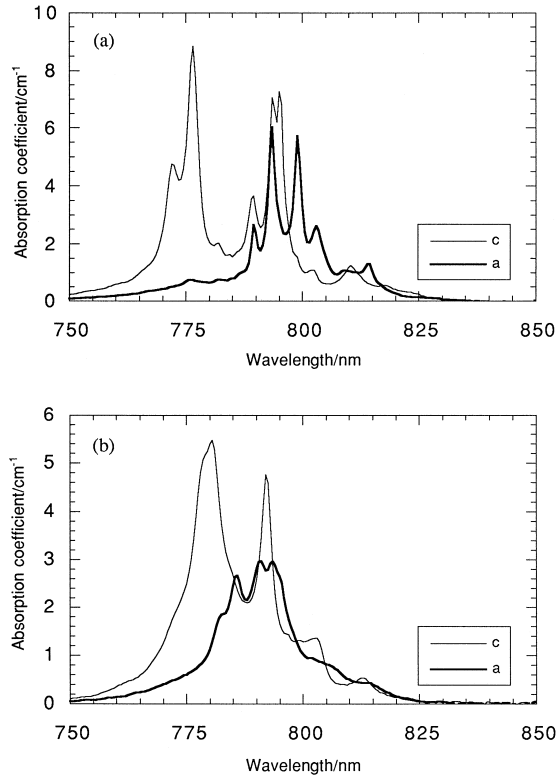

Fig. 1. Pump band absorption spectrum of (a) 4.2% thulium in YAP, and (b) 6% thulium in YLF.

the wavelength range 792 to 795 nm can access the *c*-axis absorption band peak in both materials.

On absorption of pump light to the $^3H_4$ level, the near-resonance of the $^3H_4$–$^3F_4$ and $^3H_6$–$^3F_4$ transitions results in cross-relaxation between adjacent thulium ions (one excited, the other in the ground state), efficiently populating the $^3F_4$ manifold containing the upper laser level. By this process two quanta of laser excitation are created by one pump photon. This process can be thought of as the interaction between two dipoles, representing the $^3H_4$–$^3F_4$ and $^3H_6$–$^3F_4$ transitions respectively. Hence this "two for one" process is very dependent on the separation of the thulium ions i.e. on their concentration (both Stoneman [9] and Noginov [10] quote that at least 4% Tm doping is required to make this process efficient in YAG, which corresponds to a thulium doping density of 5.6×10^{20} cm^{-3}), as well as on the degree of overlap of the emission and absorption spectra. There is rapid energy migration [11,12] amongst the thulium ions, and if holmium is also present, resonant energy transfer to the $^5I_7$ manifold can occur, de-exciting the thulium ion to the ground state. This is a reversible process, leading to a thermal equilibrium distribution of excitation between the two ions under steady-state conditions. Fig. 2 depicts the principal excitation mechanisms in thulium and holmium lasers.

Holmium does not possess an absorption transition to match the emission of GaAs/AlGaAs laser diodes hence the requirement for co-doping with thulium. A principal reason for choosing the additional complexity of double-doping is to utilise the markedly higher emission cross-sections of the holmium lasing transitions [8]. As an additional benefit, separation of pump absorption and lasing onto the two different ions allows high doping concentrations of thulium to be utilised for efficient pump beam absorption without the penalty of a prohibitively high laser threshold. The holmium doping concentration can then be kept relatively low in order to reduce the laser threshold.

With this class of laser, knowledge of the temperature distribution within the gain medium is essential not only in determining the level of thermally induced stress and lensing but also in calculating the population of the laser levels. Steady-state thermal modelling similar to that outlined by Innocenzi et al. [13] was used, assuming that 50% of the diode pump light absorbed was converted to heat. Peak temperature rises of order 25°C and 40°C were predicted for the YAP and YLF laser crystals respectively, in the experimental arrangement detailed in the next section. Assuming the first excited states of thulium and holmium to be coupled together by the excitation transfer process, in thermal equilibrium the fraction f of excited state population residing on the holmium is

$$f=\left\{1+\frac{c_{\mathrm{Tm}}Z_{\mathrm{Tm}}}{c_{\mathrm{Ho}}Z_{\mathrm{Ho}}}\exp\left(\frac{-(E_{\mathrm{Tm}}-E_{\mathrm{Ho}})}{kT}\right)\right\}^{-1}, \qquad (1)$$

where c_{Tm} (c_{Ho}), Z_{Tm} (Z_{Ho}) and E_{Tm} (E_{Ho}) are the thulium (holmium) doping concentration, partition function and first excited state lowest energy level respectively. Inspection of Eq. (1) reveals that a low $c_{\mathrm{Tm}}/c_{\mathrm{Ho}}$ ratio favours population of the holmium; however this needs to be balanced against the requirement for efficient pump absorption and low laser threshold discussed previously, conditions favoured by a large $c_{\mathrm{Tm}}/c_{\mathrm{Ho}}$ ratio. The doping concentrations used here (percentage substitution for yttrium) were 4.2% thulium (both in single and double-doped

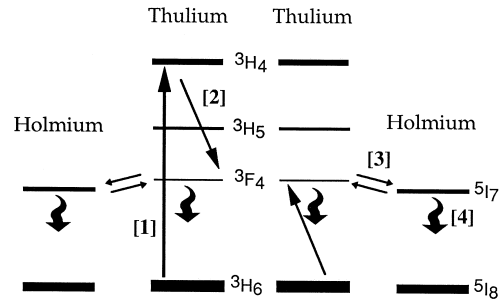

Fig. 2. Excitation mechanisms in diode-pumped two micron lasers.

crystals) and 0.28% holmium in YAP; similar number densities in YLF were achieved with doping levels of 6% thulium and 0.4% holmium. Using published data on the energy levels of thulium and holmium [14–17], the temperature distributions encountered experimentally result in approximately 55% of the excited state population residing on the holmium in both double-doped YAP and YLF. This calculation represents an upper bound on the holmium excited state population, taking no account of such phenomena as saturation of the excitation transfer process or upconversion.

In this paper, the previously reported room-temperature steady-state laser operation of Tm:YAP is expanded upon [18]. A comparison with Tm,Ho:YAP and Tm,Ho:YLF provides the majority of the results presented here. Section 2 describes the experimental arrangement employed in order to make this comparison, while in Section 3 results of output power, spectral, spatial and temporal measurements are presented and discussed.

2. Experiment

In order to overcome the lower laser level population and achieve lasing thresholds at room temperature, a high brightness pump beam is required to excite thulium and holmium lasers. This is most readily achieved by tight focussing of the laser diode output in an axial or end-pumping geometry.

The pump source for these experiments was a 500 μm aperture 3 W cw Spectra Diode Lab. Inc. laser diode, temperature tuned to either the 795 nm absorption peak of thulium in YAP, or to the 792 nm peak in YLF. Fig. 3 is a schematic of the components used. The highly divergent output of the laser diode was initially collected by a 6.5 mm focal length spherical lens, which produced an astigmatic magnified image of the diode output facet. The 40 mm focal length cylindrical lens acted to reduce the divergence of the beam in the plane perpendicular to the diode p-n junction corresponding to the wide dimension of the output facet. In this plane the divergence was many times diffraction limited. The 10 mm focal length cylindrical lens was then positioned so as to overlap its focus with the diffraction limited focus produced by the spherical lens acting in the plane perpendicular to the diode p-n junction. The inclusion of the 40 mm focal length cylindrical lens allowed a greater depth of focus to be achieved with the 10 mm lens. Using these components, a spot with FWHM size 35 by 290 μm was generated at the focal plane of the pump optics, with greater than 95% transmission through the optics train. The 35 μm dimension corresponds to the diffraction-limited portion of the diode beam, which has a confocal length of order 4 mm. From the recorded pump beam profiles, the many times diffraction-limited 290 μm spot size has an effective confocal length of at most 1 mm. Although this beam was still obviously elliptical, the aspect ratio had been significantly reduced from the rectangular dimensions of the diode output facet.

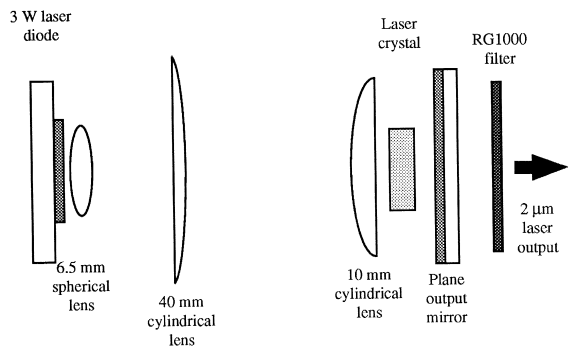

Fig. 3. Schematic of laser experimental set-up.

The laser crystals were polished plane/parallel with the pumped face coated to be highly reflecting (HR) at two microns, with high transmission of the pump beam; the other end was antireflection (AR) coated at two microns. The resonator was then completed with a flat output coupler. A range of such mirrors was available, allowing the optimum output coupling for each laser crystal to be determined. The RG1000 glass filter attenuated any unabsorbed diode light transmitted through the output mirror. Using this simple design resonators as short as 6 mm could be built. A stable resonator mode was achieved by thermal lensing in the gain medium caused by heat deposition due to absorption of the pump beam.

The laser crystals were cut axially from the boules; thicknesses available were 2 mm for Tm:YAP, 3 mm for Tm,Ho:YAP, and 4 mm for Tm,Ho:YLF. In all cases the crystals were 5 mm in cross-section, either square or circular.

3. Results and discussion

Each laser crystal was measured in turn, using the set of available mirrors in order to determine the optimum output coupling. Fig. 4 represents the best output power performance of the three types of laser crystal. Note here that the abscissa scale is incident pump power, which takes account of the transmission of the pump beam through the optics and the first face of the laser crystal. The results of this output power characterisation, including measurement of the spectral behaviour of the lasers, are listed in Table 1.

The most obvious conclusion to draw from the data plotted in Fig. 4 is the very poor performance of Tm,Ho:YAP compared to the other two lasers, both of which display comparable output power behaviour. In terms of the maximum output powers measured, the optical-to-optical conversion efficiency from diode pump light

Table 1
Summary of laser output characteristics

Crystal	Threshold pump power/W	Threshold pump intensity/kW cm^{-2}	Slope efficiency	Maximum output power/W	Output mirror transmission	Laser wavelength/μm	Polarisation
2 mm Tm:YAP	1.03	8.9	40.3	730	1.4–1.8	1.965–2.020	*a*-axis
3 mm Tm,Ho:YAP	1.06	9.2	19.3	270	2.1	2.120	*c*-axis
4 mm Tm,Ho:YLF	1.21	10.5	38.9	660	1.6	2.066	*a*-axis

to two micron laser light is 24% for Tm:YAP, 22% for Tm,Ho:YLF and 9% for Tm,Ho:YAP. These conversion efficiencies are partly determined by the transmission of the pump light through the dichroic coating on the laser crystal, the value for which is different for the three crystal types (in particular for Tm,Ho:YAP the HR coating had a measured transmission of only 81% at 795 nm). A more accurate measure of conversion efficiency uses the amount of pump light absorbed in the gain medium. The magnitude of this quantity depends on the level of stimulated emission present, as this efficiently repopulates the ground state, increasing the effective absorption coefficient from the condition where no stimulated emission is present. In the case of Tm:YAP, the absorbed pump power under lasing and nonlasing conditions was carefully measured. At maximum diode power, the absorbed pump light decreased by 14% when lasing action was inhibited. Taking this factor into account, the conversion efficiency within the laser crystals at maximum laser output was 42% for Tm:YAP, and upper bounds on the conversion efficiency of 14% for Tm,Ho:YAP and 30% for Tm,Ho:YLF were found (with the double-doped crystals the absorbed pump power was only measured under nonlasing conditions).

The temperature sensitivity of the laser transitions was observed by keeping the pump power fixed and then varying the laser crystal heatsink temperature, producing the data plotted in Fig. 5. Over this limited temperature range, a linear fit to the experimental data reveals the output power to change at -4.5 mW/°C for Tm:YAP, -7.5 mW/°C for Tm,Ho:YAP and -15.0 mW/°C for Tm,Ho:YLF. Assuming that this linear dependence can be extended to lower temperatures, it is clear that once the heatsink temperature is reduced to below 4°C, the output power of the Tm,Ho:YLF laser starts to exceed that of Tm:YAP, with Tm,Ho:YAP always lagging behind. The magnitude of this temperature-dependent behaviour is determined principally by the increase in laser threshold with temperature brought about by changes in the lower laser level population, with holmium in YLF exhibiting the greatest sensitivity because of the much reduced splitting of the ground state compared to both thulium and holmium in YAP.

It is the presence of deleterious upconversion processes which cripple the laser operation of Tm,Ho:YAP, negating the effects of the large stimulated emission cross-section. Upconversion is greater in double-doped materials than in single-doped thulium materials [19,20], and is greater in large phonon energy hosts such as YAP (740 cm^{-1} listed as the maximum phonon energy [21]) than in low phonon energy hosts such as YLF (560 cm^{-1} is maximum phonon energy in this host [22]). In the double-doped crystals, the principal upconversion mechanisms involve removing excitation from the holmium first excited state, and hence represent a loss to the two micron laser transition. Fig. 6 depicts these upconversion mechanisms. One process involves absorption of pump light from holmium $^5I_7$, which leads to the production of visible upconversion fluorescence. This represents only a small fraction of the total upconversion, the majority of which arise from a thulium-holmium interaction whereby a thulium ion de-excites ($^3F_4$–$^3H_6$), promoting an excited state holmium ($^5I_7$–$^5I_5$). From $^5I_5$ fluorescence can occur centred at approximately

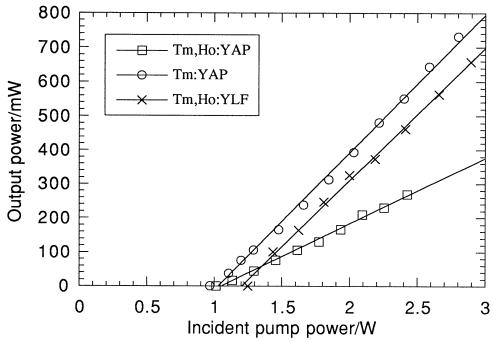

Fig. 4. Best output power performance of the three lasers.

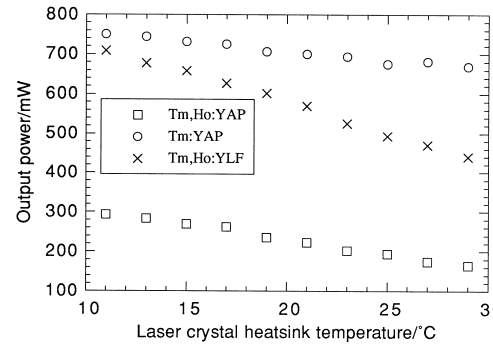

Fig. 5. Comparison of temperature dependence of output power.

900 nm; in YAP this level is strongly quenched by nonradiative decay. Therefore with Tm,Ho:YAP a large fraction of the upconverted excitation decays nonradiatively into the host lattice providing additional heating and subsequent degradation of the laser performance. The importance of the holmium $^5I_7$ first excited state to the visible upconversion process is clearly demonstrated by the noticeable decrease in the brightness of the upconversion fluorescence, as viewed by the naked eye, at the onset of stimulated emission.

Measurement of the fluorescence decay lifetime of the coupled first excited states of Tm,Ho:YAP and Tm,Ho:YLF provided further evidence of the presence of upconversion. Using the same laser diode and pump optics as during the laser experiments, but now running the diode in pulsed rather than cw mode, the fluorescence from each of the crystal types was captured by a lens and focussed, after filtering any unabsorbed diode light, onto a long wavelength InGaAs photodiode. Diode pump pulses of 1 ms duration were used in order to provide detectable fluorescence signals, combined with the use of a preamplifier. The 5 cm focal length $f/1$ collection lens was stopped down with a 5 mm aperture in order to provide a 1 mm depth of focus within the laser crystal. The observed decay profiles were not single exponential, but rather consisted of an initial nonexponential decay which was faster at higher pump intensities, with a slow exponential tail independent of the incident intensity. The intensity-dependent portion of the decay was indicative of the thulium-holmium upconversion process. In Tm,Ho:YAP, the initial nonexponential decay was measured to have an effective lifetime increasing from 2.1 to 4.0 ms as the incident pump intensity decreased from 21 to 2.3 kW cm^{-2} using neutral density filters, while the exponential tail had a lifetime of 4.8 ± 0.3 ms. This exponential portion of the total decay is a measure of the lifetime of the coupled thulium and holmium first excited states. As the incident pump intensity decreases, the magnitude of the upconversion is reduced, and the total fluorescence decay becomes closer to a single exponential in nature. Typical decay profiles are shown in Fig. 7. With Tm,Ho:YLF, the initial nonexponential decay increased from 6.9 to 12.0 ms as the incident pump intensity decreased, with an exponential tail of lifetime 12.4 ± 0.1 ms. This decrease in the upconversion as the pump intensity is reduced is more marked than in the YAP, and combined with the higher incident intensities experienced by the YLF crystal (higher transmission of laser crystal HR coating at pump wavelength), is taken to indicate that the holmium $^5I_7$ to $^5I_5$ upconversion is weaker in YLF than in YAP. Armagan et al. [23] reported that a comparison of Tm,Ho:YAG and Tm,Ho:YLF with similar dopant concentrations showed upconversion losses to be greater in the former. The negligible upconversion rate in Tm:YAP was confirmed by measuring a single exponential fluorescence decay lifetime of 4.4 ± 0.2 ms, independent of the pump intensity, as shown in Fig. 8.

The presence of upconversion also manifested itself when measuring the amount of pump light absorbed in the laser crystals. For single-doped Tm:YAP, intensity-depen-

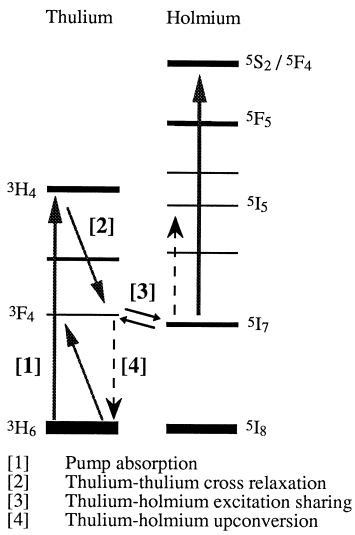

Fig. 6. Principal upconversion mechanisms in double-doped materials.

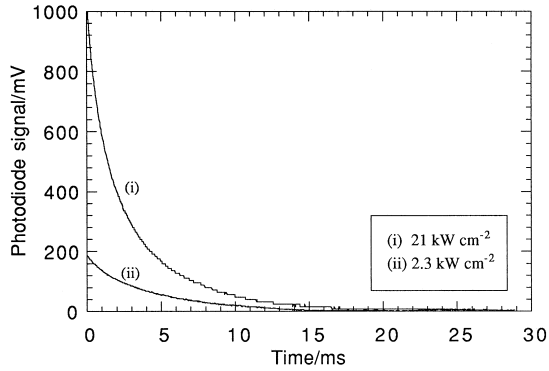

Fig. 7. Intensity-dependent fluorescence decay profiles of Tm,Ho:YAP.

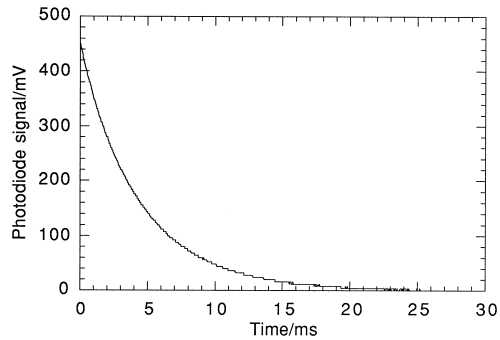

Fig. 8. Infrared fluorescence decay of Tm:YAP.

dent bleaching of the ground state population, as investigated in several papers [24,25], is the main contribution to the observed pump absorption behaviour. Significant bleaching of the thulium ground state was measured. Under nonlasing conditions at maximum pump power 1.2 W of pump was observed to be transmitted through the 2 mm thick crystal, while a transmitted signal of only 765 mW was expected from the measured thulium absorption coefficient (Fig. 1), taken in conjunction with the diode linewidth and transmission of the HR and AR coated crystal faces at the pump wavelength. In Tm,Ho:YAP the additional pump beam absorption from the holmium first excited state, combined with the thulium-holmium upconversion which repopulates the thulium ground state (referring back to Fig. 6), act in opposition to the bleaching process, and in effect almost completely negate it. A similar effect was also observed in Tm,Ho:YLF.

The wavelength and polarisation of the laser output is determined by which particular transition reaches threshold first. In general this tends to be the longest wavelength possible, as this corresponds to the transition terminating in the highest level of the ground state which is the level containing the smallest fraction of the ground state population. For the Tm:YAP laser the output wavelength was not a fixed value, but instead varied over the range 1.965 to 2.020 μm, depending on which particular output mirror was used. When the output mirror was changed, the laser changed wavelength such that the output coupling was always in the range 1.4 to 1.8%T, in all cases yielding the output power behaviour shown in Fig. 4. Furthermore, the output spectrum consisted of a comb of wavelengths, the separation of which was several nanometres, much larger than the 19.2 GHz (0.25 nm) longitudinal mode separation of the resonator. These lines were all polarised parallel to the YAP *a*-axis. The number of lines lasing at any one time varied from two to ten, depending critically on the resonator length and alterations in alignment. Opening the output slit of the monochromator (Bentham M300HRA) to allow all the lasing lines to be viewed simultaneously, a typical spectrum as captured by a thermal imager camera

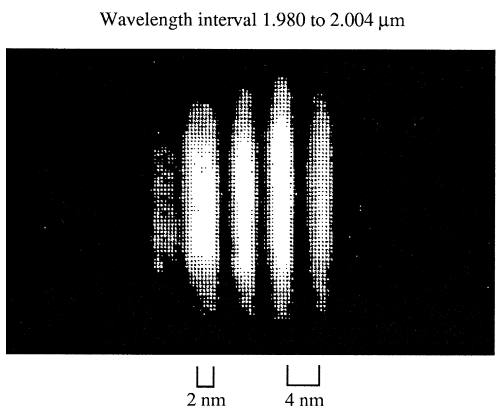

Fig. 9. Representative wavelength spectrum of Tm:YAP laser.

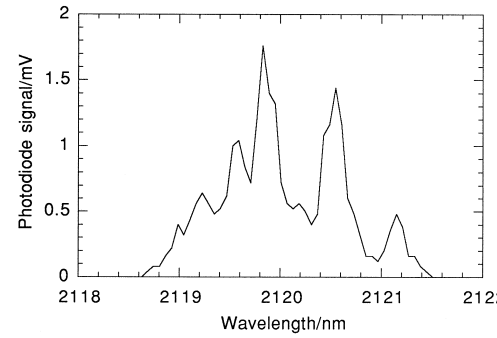

Fig. 10. Spectrum of Tm,Ho:YAP laser ouptput.

is shown in Fig. 9. The intensity of individual lines varied with time, one line or several lines decreasing in strength as others increased. With no intracavity line-narrowing element, the broad bandwidth of the thulium gain (a measure of which is given by the room-temperature fluorescence spectrum of Tm:YAP which extends continuously from 1600 to 2000 nm [26]) allowed a series of lines to lase. Any feedback from AR coated surfaces e.g. the unwedged back surface of the output mirror, can lead to multiple etalon effects within the laser, which will be supported by the broad gain spectrum. The presence of multiple etalons restricts operation to modes which match all the etalons simultaneously. This is an inherently unstable mode of operation, as any changes in resonator length will alter the overlap between the various etalons present, in turn changing the output spectrum. Changes in the resonator length can be caused by mechanical perturbations, by temperature changes, and also by fluctuations in the diode pump beam altering the heat load in the laser crystal causing its degree of thermal expansion to vary. The inherently low emission cross-section of the thulium makes the lasing transition very sensitive to any perturbations of the lasing mode, which exacerbates the instabilities introduced by the multiple etalons present. This instability rendered it impossible to analyse these effects quatitatively. Similar broadband laser output behaviour occurs in Ti:sapphire lasers if no intracavity line-narrowing occurs [27,28].

In the case of Tm,Ho:YAP, a typical wavelength spectrum is plotted in Fig. 10. The lasing output is centred on 2.12 μm, corresponding to the transition from the closely-spaced lowest two levels of the holmium $^5I_7$ first excited state to the second from highest level of the $^5I_8$ ground state. The longitudinal mode structure of the laser output is partially resolved by this measurement, revealing a FWHM of just over 1 nm. By interrogating the laser output with a 135 GHz plane-plane scanning Fabry-Perot interferometer (Burleigh RC140), the longitudinal mode structure of the output spectrum can be viewed, as in Fig. 11. The Tm,Ho:YAP laser ran typically on six longitudinal modes (the Fabry-Perot mirrors were not designed for operation at this wavelength, and so the instrument finesse was low, as

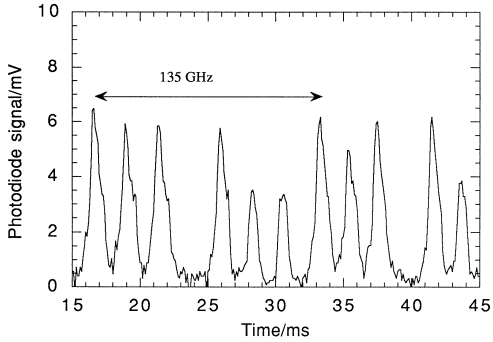

Fig. 11. Fabry-Perot trace of Tm,Ho:YAP laser output.

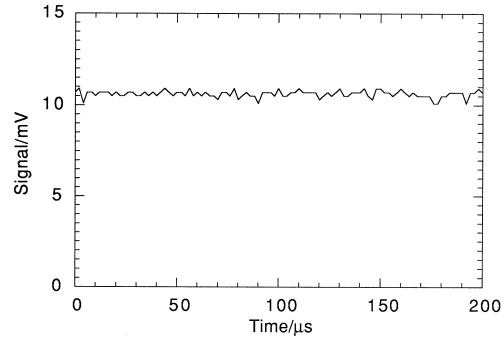

Fig. 13. Typical temporal bahaviour of Tm,Ho:YAP laser.

evidenced by the width of the recorded fringes). In similar fashion the output spectrum of the Tm,Ho:YLF laser was recorded, and is shown in Fig. 12. The output is centred on 2.066 μm, corresponding to a transition from the lowest three levels of the holmium $^5I_7$ first excited state to the two highest lying levels of the $^5I_8$ ground state. The FWHM of this spectrum is 3 nm which, at 210 GHz, is wider than the free spectral range of the Fabry-Perot interferometer, thus preventing a definitive measurement of the longitudinal mode structure. Strong spatial holeburning effects in the two-mirror standing wave resonator employed here allow multilongitudinal mode operation of both Tm,Ho:YAP and Tm,Ho:YLF.

By transforming the output of each laser through a lens and looking at the far-field propagation, in each case the beam was found to be near diffraction-limited, within the accuracy of the beam profile measurements made. Misalignment of the resonator extinguished lasing without allowing operation on higher order transverse modes. The unpumped region of the gain medium surrounding the pumped volume acted as a very lossy element to the laser emission, behaving in effect as a ''soft'' aperture. With the use of a plane output coupler, it is the thermal lensing in the gain medium that allows a stable resonator mode to be formed. The magnitude of the thermal lens determines the size and shape of the resonator mode, which forms a beam waist at the output mirror. A stronger thermal lens is equivalent to a mirror with a shorter radius of curvature, producing a smaller beam waist at the output mirror. This manifested itself in the laser output as a more highly divergent beam. Using the measurements of absorbed pump power in the laser crystals, the thermal modelling calculations were used to estimate the thermal lensing, taking into account that the laser mode ''sees'' the thermally induced lens in the birefringent gain medium which corresponds to the polarisation of the laser radiation. Thermal lens of focal lengths 3 cm in Tm,Ho:YAP, 5 cm in Tm:YAP and 10 cm in Tm,Ho:YLF were derived in this fashion; their relative strengths were confirmed by observation of the near-field beam divergence of each laser. It is worth noting that the short resonator lengths employed in these laser experiments allowed the Tm,Ho:YLF to operate on an *a*-axis polarised transition, with thermal lensing almost an order of magnitude stronger than if the laser radiation was polarised parallel to the *c*-axis.

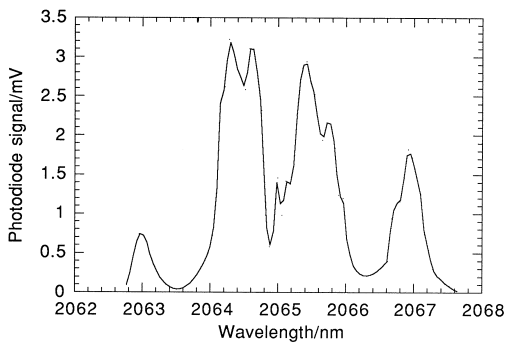

Fig. 12. Spectrum of Tm,Ho:YLF laser output.

Monitoring the output of these lasers with a long wavelength InGaAs photodiode revealed a marked difference between the temporal behaviour of the single and double-doped crystals. A typical oscilloscope trace of the output of the Tm,Ho:YAP laser is shown in Fig. 13, which would also equally well apply to Tm,Ho:YLF. The timescale viewed is not short enough to see any intensity fluctuations in the laser output due to longitudinal mode-beating effects. The observed behaviour is that expected for steady-state operation, with the small fluctuations on the otherwise flat photodiode signal due to detector noise.

Repeating this measurement with the Tm:YAP laser produced a markedly different result, as shown in Fig. 14. The expected flat photodiode signal is instead dominated by a continuous series of spikes, the amplitude envelope of which varies over time in what appears to be a nonrepeatable fashion [1]. Inspection of this trace shows that large amplitude spiking behaviour can damp down to lower levels, but never decays to small-signal relaxation oscilla-

[1] When viewed on an analogue oscilloscope, the spikes are smooth in lineshape. Any distortions evident here are due to the digitisation process in the oscilloscope used to record these traces.

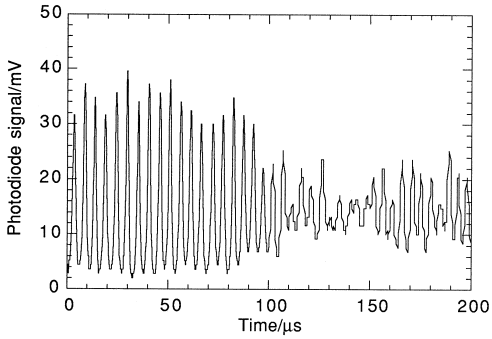

Fig. 14. Example of recorded temporal behaviour of Tm:YAP laser.

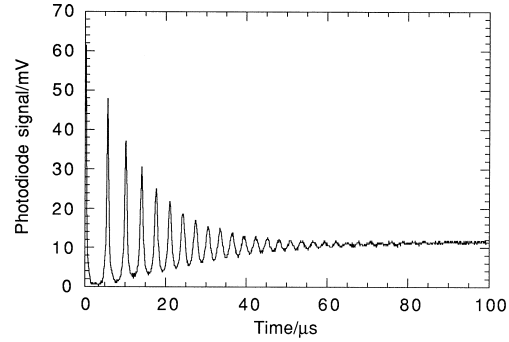

Fig. 15. Spiking/relaxation oscillations in Tm,Ho:YAP.

tions or to true cw operation before the spiking amplitude grows again. The recorded trace shows that as the spike amplitude decreases the period of the spiking also decreases while the width of the spikes increases, which is characteristic of the spiking/relaxation oscillation behaviour expected in solid-state lasers [29]. Spiking behaviour dominated the laser output intensity independent of how far the laser operated above threshold.

Feedback effects were considered as potential sources of this intensity instability. However, use of an optical isolator to prevent feedback of the Tm:YAP laser output back into the resonator made no difference to the observed temporal behaviour. Feedback of diode pump light reflected from the pumped face of the Tm:YAP laser back into the laser diode was effectively suppressed with the insertion of a polariser and quarter-wave plate in the pump optics train. Again, there was no detectable change in the temporal behaviour of the Tm:YAP laser. It was known that feedback into the diode introduced intensity fluctuations onto the pump beam, and although these may have contributed to the resultant instability in the thulium laser output, the observed behaviour meant that this was only a minor effect.

As has already been discussed, the Tm:YAP laser was observed to operate on a series of distinct wavelengths. This multi-line operation, with its high degree of instability, was also considered as a potential driving mechanism producing spiking behaviour in the time domain. Increasing the resonator length to allow introduction of a 27 μm thick uncoated fused silica etalon, the output spectrum was reduced to a single line. However, the temporal behaviour of the laser was unchanged, save for a slight increase in the spiking period due to the insertion loss of the etalon raising the laser threshold.

Returning to the double-doped lasers, perturbation of the resonator would be expected to give rise to some form of spiking in the laser output intensity. With the Tm,Ho:YAP laser, tapping the output mirror mount induced a set of spikes which damped back down to the steady-state intensity within a 100 μs interval. Similar results were obtained by driving the laser diode in pulsed rather than cw mode. In this mode of operation, holmium laser output pulses were generated with a set of spikes at the leading edge, a typical example of which is shown in Fig. 15. The single set of large amplitude spikes decays to small-signal relaxation oscillations and finally to steady-state operation within 100 μs, markedly different behaviour than the Tm:YAP laser. Tm,Ho:YLF was found to behave in a similar fashion to Tm,Ho:YAP.

Siegman [29] provides an analysis of relaxation oscillations for the case of an ideal four-level laser, based on the original work of Kleinman [30]. The starting equations for this analysis are the rate equations for the population inversion density and the intracavity photon number density. Analytical solutions to the rate equations for this class of laser are not trivial to derive in the case where stimulated emission is present. Instead it is proposed to state the starting equations, and then by comparison with the full solution for the four-level laser obtain the corresponding damping rate. Fig. 16 depicts the principal mechanisms that need to be considered for lasing in both thulium and thulium, holmium lasers.

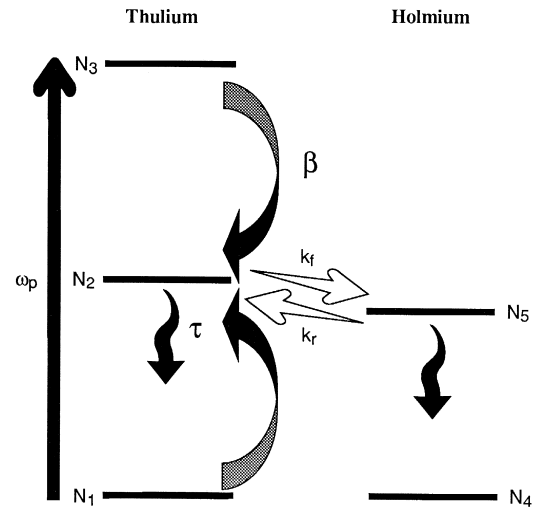

Fig. 16. Principal parameters used in relaxation oscillation analysis.

The starting equations for the four-level laser analysis are the rate equations for the population inversion density ΔN and the intracavity photon number density n

$$\frac{\mathrm{d}\Delta N}{\mathrm{d}t} = R_\mathrm{p} - \Delta N n \sigma c - \frac{\Delta N}{\tau}, \tag{2a}$$

and

$$\frac{\mathrm{d}n}{\mathrm{d}t} = \Delta N n \sigma c - \gamma_\mathrm{c} n. \tag{2b}$$

where R_p is the pump rate, σ is the emission cross-section, τ is the lifetime of the upper laser level and γ_c is the cavity decay rate.

Considering first the case of a thulium laser, we assume that the total thulium population density N_Tm resides in the three levels of Fig. 16 (corresponding to the $^3\mathrm{H}_6$, $^3\mathrm{F}_4$ and $^3\mathrm{H}_4$ energy level manifolds), yielding

$$N_\mathrm{Tm} = N_1 + N_2 + N_3. \tag{3}$$

The rate equations for the level population densities of this system are

$$\frac{\mathrm{d}N_3}{\mathrm{d}t} = \omega_\mathrm{p} n_1 - \beta N_1 N_3, \quad \frac{\mathrm{d}N_2}{\mathrm{d}t} = 2\beta N_1 N_3 - \frac{N_2}{\tau} - N n \sigma c, \tag{4}$$

where ω_p is the pump rate and β is the cross-relaxation parameter. The rate equation for the photon number density is as before

$$\frac{\mathrm{d}n}{\mathrm{d}t} = \Delta N n \sigma c - \gamma_\mathrm{c} n. \tag{5}$$

The population inversion density on the thulium laser transition is defined as

$$\Delta N = f_u N_2 - f_l N_1, \tag{6}$$

where $f_u(f_l)$ is the temperature-dependent fractional occupation of the upper (lower) laser level, yielding the with corresponding rate equation

$$\begin{aligned}\frac{\mathrm{d}\Delta N}{\mathrm{d}t} &= f_u \frac{\mathrm{d}N_2}{\mathrm{d}t} - f_l \frac{\mathrm{d}N_1}{\mathrm{d}t} \\ &= -(f_u + f_l)\Delta N n \sigma c - (f_u + f_l)\frac{N_2}{\tau} \\ &\quad + f_l \omega_\mathrm{p} N_1 + (2 f_u + f_l)\beta N_1 N_3.\end{aligned} \tag{7}$$

Eliminating N_3 and N_1 from this equation, and expressing N_2 in terms of the population inversion, we obtain the following

$$\begin{aligned}\frac{\mathrm{d}\Delta N}{\mathrm{d}t} &= \left[2 f_u \omega_\mathrm{p}\left(N_\mathrm{Tm} + \frac{f_l}{2 f_u \beta \tau} - \frac{\Delta N}{f_u} - \frac{\omega_\mathrm{p}}{\beta}\right) - \frac{f_l}{\tau} N_\mathrm{Tm}\right] \\ &\quad - (f_u + f_l)\Delta N n \sigma c - \frac{\Delta N}{\tau}.\end{aligned} \tag{8}$$

Eqs. (5) and (8) serve as the starting equations for the relaxation oscillation analysis, to be compared with Eqs. (2a) and (2b) for a four-level laser. The term inside the square brackets represents the pumping rate taking into consideration the need for a minimum pump rate in order to generate a population inversion. Therefore by inspection the resulting linearised small-signal analysis will lead to an expression for the damping rate γ_osc (using similar notation to Siegman) which is identical to the four-level laser case i.e.

$$\gamma_\mathrm{osc} = \frac{r}{2\tau}, \tag{9}$$

where r is the pumping ratio.

For the double-doped thulium, holmium laser the population inversion now occurs on the holmium. Making the assumption that the total holmium population density N_Ho is restricted to the ground and first excited states only, the full set of rate equations for the population densities of this system are

$$\begin{aligned}\frac{\mathrm{d}N_3}{\mathrm{d}t} &= \omega_\mathrm{p} N_1 - \beta N_1 N_3, \\ \frac{\mathrm{d}N_2}{\mathrm{d}t} &= 2\beta N_1 N_3 - \frac{N_2}{\tau} - k_f N_2 N_4 + k_r N_5 N_1, \\ \frac{\mathrm{d}N_5}{\mathrm{d}t} &= k_f N_2 N_4 - k_r N_5 N_1 - \frac{N_5}{\tau} - \Delta N n \sigma c = -\frac{\mathrm{d}N_4}{\mathrm{d}t},\end{aligned} \tag{10}$$

where $k_f(k_r)$ is the forward (reverse) excitation transfer parameter. The photon number density rate equation identical to Eq. (2b).

The resulting rate equation for the population inversion on the holmium laser transition is

$$\begin{aligned}\frac{\mathrm{d}\Delta N}{\mathrm{d}t} &= -(f_u + f_l)\Delta N n \sigma c - (f_u + f_l)\frac{N_5}{\tau} \\ &\quad + (f_u + f_l)(k_f N_2 N_4 - k_r N_5 N_1).\end{aligned} \tag{11}$$

The final term in the above equation represents the pump rate into the holmium. Explicitly it appears as though it is determined solely by the net excitation sharing rate. Implicitly it depends on the pump rate into the thulium through the N_1 and N_2 terms. Expressing N_4 and N_5 in terms of the population inversion density yields

$$\begin{aligned}\frac{\mathrm{d}\Delta N}{\mathrm{d}t} &= N_\mathrm{Ho}\left((f_u k_f N_2 - f_l k_r N_1) - \frac{f_l}{\tau}\right) \\ &\quad - (f_u + f_l)\Delta N n \sigma c - \Delta N\left(\frac{1}{\tau} + k_f N_2 + k_r N_1\right).\end{aligned} \tag{12}$$

Comparing this with Eq. (2a) the damping rate is given by

$$\gamma_\mathrm{osc} = \frac{r}{2\tau_\mathrm{d}}, \tag{13}$$

where

$$\frac{1}{\tau_\mathrm{d}} = \frac{1}{\tau} + (k_f N_2 + k_r N_1). \tag{14}$$

This rate equation analysis reveals the reason for the

different temporal behaviour of thulium and thulium, holmium lasers. In the case of the latter, in addition to the fluorescence lifetime of the upper state, the excitation transfer rate between the thulium and holmium needs to be considered when studying relaxation oscillation phenomena.

As previously mentioned, the fluorescence lifetime of the thulium $^3F_4$ first excited state in YAP was measured to be 4.4 ms. This long lifetime results in very weak damping of any spiking in the laser output. For a single set of spikes, it will take of order 40 to 50 ms for the laser output to return to steady-state oscillation. Any further perturbations to the resonator within this period will result in another set of spikes appearing before the initial set have decayed, with the cumulative effect that the expected cw output is instead dominated by large amplitude spiking. It is proposed that the low-gain thulium laser transition is very sensitive to mechanical or acoustic perturbations to the laser resonator, which occur at frequencies up to a few kilohertz, resulting in the highly unstable temporal behaviour observed.

Pulsed operation of the Tm,Ho:YAP laser allowed the decay rate of the relaxation oscillations to be measured (Fig. 15). In this pulsed mode, the laser operated at twice threshold with the diode output at its maximum. Fitting an exponential decay of the form $\exp(-\gamma_{osc}t)$ to the recorded relaxation oscillations, and taking into account how far the laser was from threshold, a value for τ_d of 11.9 ± 0.8 μs was obtained. This value is the sum of the contributions from both the fluorescence decay and the excitation sharing. The effective fluorescence lifetime of the coupled thulium and holmium first excited states was measured to be 2.7 ms, nearly three orders of magnitude larger than τ_d. Therefore the value of τ_d can be equated to the effective lifetime of the excitation transfer process between thulium and holmium. Carrying out a similar analysis for Tm,Ho:YLF, which in pulsed mode was operated at up to 1.5 times threshold, a value for τ_{-d} of 14.8 ± 1.2 μs was obtained.

From the open literature, the characteristic lifetime of excitation transfer in Tm,Ho:YAG was calculated as being in the range 10 to 20 μs, where the rare earth concentrations were comparable with the doping levels in both the Tm,Ho:YAP and Tm,Ho:YLF crystals used here [31]. In this case the magnitude of the excitation transfer rate was derived from spectroscopic measurements of the fluorescence of the first excited states of thulium and holmium. Therefore it is proposed that the excitation transfer between thulium and holmium acts as a strong damping mechanism, rapidly quenching any spiking or relaxation oscillations induced by perturbations to the lasing mode. The work of Becker and Huber [32,33] indicated that in flashlamp-pumped Tm:YAG and Tm,Ho:YAG, the latter exhibited much reduced spiking behaviour, which the authors attributed to the excitation sharing in the double-doped laser crystal.

4. Conclusions

A comparison of the room-temperature cw laser performance of Tm:YAP, Tm,Ho:YAP and Tm,Ho:YLF has been made. In terms of conversion efficiency from absorbed pump power to laser output, Tm:YAP offered the superior performance (42%), generating 730 mW of laser output, compared with 14% conversion efficiency in Tm,Ho:YAP (270 mW maximum output) and 30% in Tm,Ho:YLF (660 mW maximum output). The performance of Tm,Ho:YLF, demonstrating a slope efficiency of 38.9% and an optical-to-optical conversion efficiency of 22%, is superior to the room temperature operation reported by McGuckin et al. [34], where the slope efficiency was 17% with a corresponding conversion efficiency 11.5%. It also compares well with the reported work of Budni et al. [35], where Tm,Ho:YLF cooled to 77 K demonstrated a slope efficiency of 49.4% and an optical-to-optical conversion efficiency of 45.6%. Here the reduced temperature of the gain medium acted principally to decrease the laser threshold.

With the use of an AlGaAs laser diode operating at around 795 nm as the pump source, lasing utilising the higher gain transitions on holmium required co-doping with thulium. This reduced the achievable efficiency because excitation had to be shared between the two ions. Double-doping also introduced significant levels of upconversion which was deleterious to the lasing process. This was especially the case with Tm,Ho:YAP, where a large fraction of the upconverted excitation decayed nonradiatively, producing additional heating of the crystal and subsequently further degrading the achievable laser performance. The presence of upconversion, and its greater strength in YAP than YLF, was confirmed by observing the intensity-dependent fluorescence decay lifetime of the coupled thulium and holmium first excited states. These additional upconversion processes in the double-doped laser crystals were found to counteract the pump beam bleaching of the thulium ground state observed in Tm:YAP by repopulating the thulium ground state. Tm:YAP was measured to have the output power least sensitive to changes in the laser crystal temperature, a direct measure of the relative population of the lower laser level. All three lasers were observed to operate on the fundamental transverse mode.

However, the Tm:YAP laser was observed to operate on a comb of lines in the range 1.965 to 2.020 μm. This wide spectral output was attributed to multiple etalon effects within the laser resonator, supported by the wide gain bandwidth of thulium. In contrast, both of the holmium lasers operated reliably on a single transition, at wavelengths of 2.066 and 2.120 μm respectively for Tm,Ho:YLF and Tm,Ho:YAP.

In the time domain the output of the Tm:YAP laser was dominated by fluctuations characteristic of spiking/relaxation oscillation behaviour, whereas both Tm,Ho:YAP and

Tm,Ho:YLF displayed the expected smooth output intensity behaviour. A rate equation analysis showed that in the double-doped materials, strong damping of any fluctuations on the lasing mode occurred due to the relatively rapid excitation sharing process between the thulium and holmium first excited states. With Tm:YAP, it was solely the long fluorescence lifetime (measured to be 4.4 ms) of the upper laser level that provided any damping, which as a consequence was very weak. Preliminary experiments by these authors with a diode-pumped Tm:YAG laser (results to be published elsewhere) have shown that the output of this laser also suffers from spiking fluctuations, but not to the same degree as in Tm:YAP. In addition, the Tm:YAG did not operate on as wide a comb of wavelengths, indeed often running single line. Clearly further investigation of both Tm:YAP and Tm:YAG is merited, but it is apparent that the broad gain bandwidth and low gain cross-section inherent to the thulium ion render it very sensitive to perturbations of the lasing mode, a problem overcome in double-doped thulium, holmium lasers.

Acknowledgements

The authors would like to thank Brian Cockayne, Mick Crosbie and Leslie Taylor for growth of the YAP and YLF boules; Roy Vivian and Steve Aldridge for cutting and polishing the laser samples.

References

[1] M. Storm, Laser Focus World, April 1991.
[2] B. Ropoulos, Photonics Spectra, June 1996.
[3] J.G. Manni, Optics and Photonics News, July 1996.
[4] J.G. Manni, Lasers and Optronics, April 1992.
[5] S.R. Bowman, J.G. Lynn, S.K. Searles, B.J. Feldman, J. McMahon, W. Whitney, D. Epp, G.J. Quarles, K.J. Riley, Opt. Lett. 18 (1993) 1724.
[6] L.A. Pomeranz, P.A. Budni, P.G. Schunemann, T.M. Pollak, E.P. Chicklis, in: Technical Digest of Advanced Solid-State Lasers (OSA, Washington, DC, 1997) p. 226.
[7] R.J. Pressley, CRC Handbook of Lasers with Selected Data on Optical Technology, CRC Press, Ohio, 1971.
[8] S.A. Payne, L.L. Chase, L.K. Smith, W.L. Kway, W.F. Krupke, IEEE J. Quantum Electron. 28 (1992) 2619.
[9] R.C. Stoneman, L. Esterowitz, Opt. Lett. 17 (1992) 736.
[10] M.A. Noginov, A.M. Prokhorov, G.K. Sarkisyan, V.A. Smirnov, I.A. Shcherbakov, Sov. J. Quantum Electron. 21 (1992) 945.
[11] V.A. Fenach, R.C. Powell, Opt. Lett. 16 (1991) 666.
[12] S.A. Payne, L.K. Smith, W.L. Kway, J.B. Tassano, W.F. Krupke, J. Phys. Condens. Matter 4 (1992) 8525.
[13] M.E. Innocenzi, H.T. Yura, C.L. Fincher, R.A. Fields, Appl. Phys. Lett. 56 (1990) 1831.
[14] H.P. Jenssen, A. Linz, R.P. Leavitt, C.A. Morrison, D.E. Wortman, Phys. Rev. B 11 (1975) 92.
[15] J.M. O'Hare, V.L. Donlan, Phys. Rev. B 14 (1976) 3732.
[16] N. Karayianis, D.E. Wortman, H.P. Jenssen, Phys. Chem. Solids 37 (1976) 675.
[17] A.A. Kaminskii, Laser Crystals, 2nd ed., Springer-Verlag, Berlin, 1990.
[18] I.F. Elder, M.J.P. Payne, Diode-pumped, room-temperature Tm:YAP laser, to be published in Applied Optics 36 (1997).
[19] T.Y. Fan, G. Huber, R.L. Byer, P. Mitzscherlich, IEEE J. Quantum Electron. 24 (1988) 924.
[20] M. Falconieri, A. Lanzi, G. Salvetti, Appl. Phys. B 62 (1996) 537.
[21] M.J. Weber, Phys. Rev. B 8 (1973) 54.
[22] T.T. Basiev, Y.V. Orlovskii, K.K. Pukhov, V.B. Sigachev, M.E. Doroshenko, I.N. Vorob'ev, in: Advanced Solid-State Lasers, OSA Trends in Optics and Photonics Series, vol. 1 (OSA, Washington, DC, 1996) p. 575.
[23] G. Armagan, A.M. Buoncristiani, A.T. Inge, B. DiBartolo, in: Advanced Solid-State Lasers, OSA Proceedings Series, vol. 10 (OSA, Washington, DC, 1991) p. 222.
[24] C. Hauglie-Hanssen, N. Djeu, IEEE J. Quantum Electron. 30 (1994) 275.
[25] P. Peterson, A. Gavrielides, M.P. Sharma, Appl. Phys. B 61 (1995) 195.
[26] I.F. Elder, M.J.P. Payne, in: Advanced Solid-State Lasers, OSA Proceeding Series, vol. 15 (OSA, Washington, DC, 1995) p. 358.
[27] N.J. Vasa, M. Tanaka, T. Okada, M. Maeda, O. Uchino, Appl. Phys. B 62 (1996) 51.
[28] V.I. Donin, V.A. Ivanov, V.I. Kovalevskii, D.V. Yakovin, Optics Comm. 122 (1995) 40.
[29] A.E. Siegman, Lasers (University Science Books, 1986) principally Ch. 25.
[30] D.A. Kleinman, Bell Sys. Tech. J. 43 (1964) 1505.
[31] R.R. Petrin, M.G. Jani, R.C. Powell, M. Kokta, Optical Materials 1 (1992) 111.
[32] T. Becker, G. Huber, in: Conference on Lasers and Electro-Optics, vol. 11, OSA Technical Digest Series (OSA, Washington, DC, 1991) paper CTuO3.
[33] T. Becker, G. Huber, J. Phys. IV Coll. 1 (1991) 353.
[34] B.T. McGuckin, R.T. Menzies, H. Hemmati, Appl. Phys. Lett. 59 (1991) 2926.
[35] P.A. Budni, M.G. Knights, E.P. Chicklis, H.P. Jenssen, IEEE J. Quantum Electron. 28 (1992) 1029.